

AD-A097 299

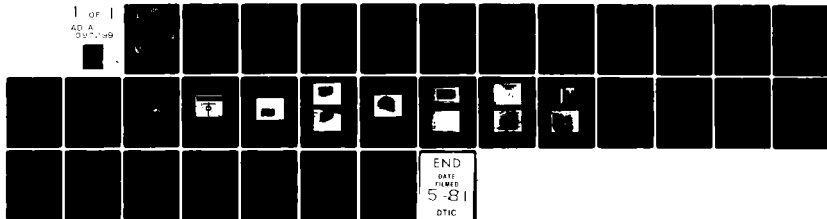
ARMY MISSILE COMMAND REDSTONE ARSENAL AL GROUND EGU--ETC F/6 14/5
ACOUSTICAL HOLOGRAPHIC RECORDING WITH COHERENT OPTICAL READ-OUT--ETC(U)
OCT 80 H LIU
DRSMI/RL-81-2-YR

UNCLASSIFIED

SBIE-AD-E950 106

NL

1 OF 1
AD A
007-199



(12) LEVEL III AD-E 950106

AD A 097299



TECHNICAL REPORT RL-81-2

ACOUSTICAL HOLOGRAPHIC RECORDING WITH
COHERENT OPTICAL READ-OUT AND IMAGE PROCESSING

Hua-Kuang Liu
Ground Equipment and Missile Structures Directorate
US Army Missile Laboratory

3 October 1980

DTIC
ELECTE
S APR 3 1981 D
B

Approved for public release; distribution unlimited.



U.S. ARMY MISSILE COMMAND
Redstone Arsenal, Alabama 35898

DTIC FILE COPY

81 3 23 085

DISPOSITION INSTRUCTIONS

**DESTROY THIS REPORT WHEN IT IS NO LONGER NEEDED. DO NOT
RETURN IT TO THE ORIGINATOR.**

DISCLAIMER

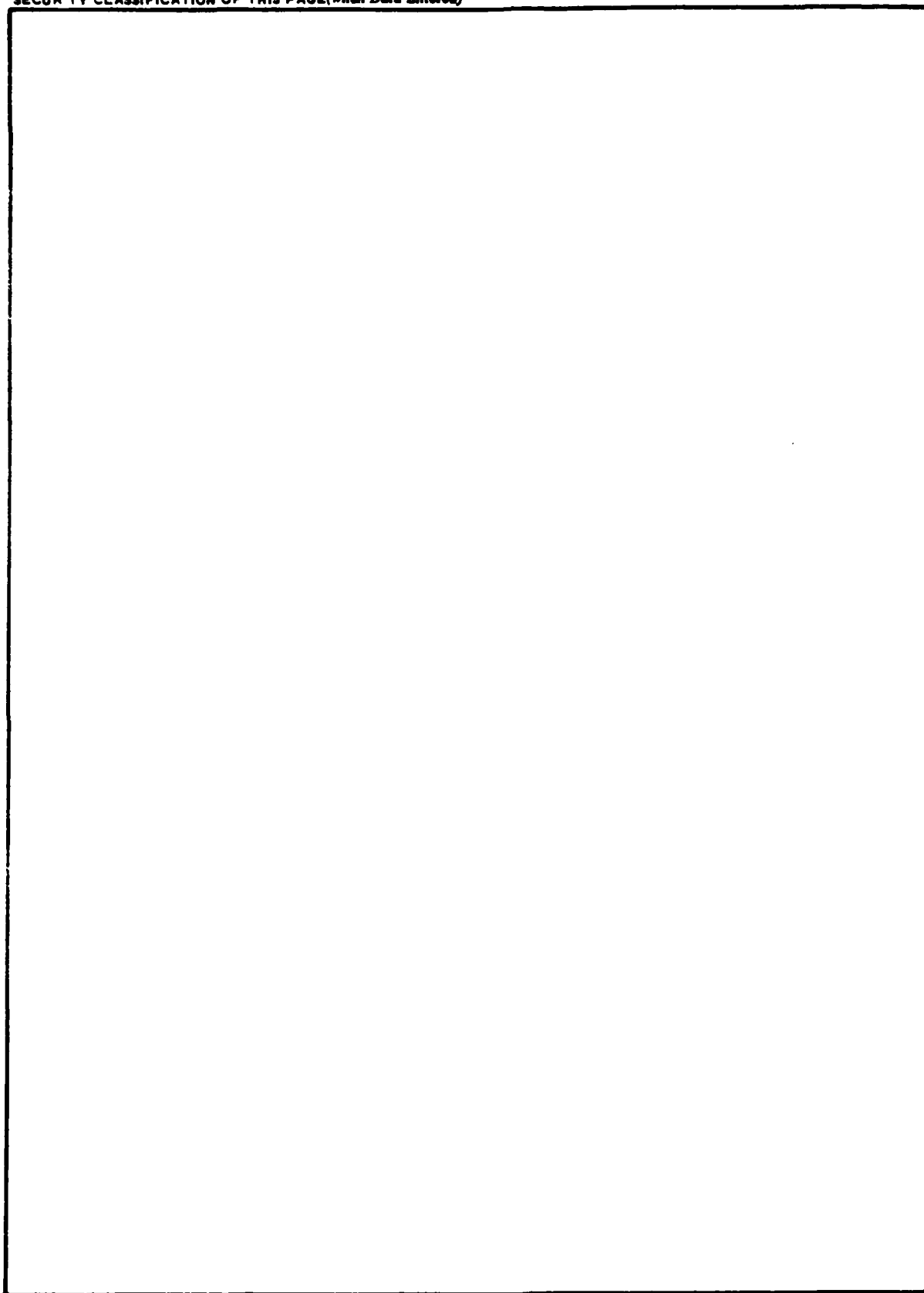
**THE FINDINGS IN THIS REPORT ARE NOT TO BE CONSTRUED AS AN
OFFICIAL DEPARTMENT OF THE ARMY POSITION UNLESS SO DESIGNATED
BY OTHER AUTHORIZED DOCUMENTS.**

TRADE NAMES

**USE OF TRADE NAMES OR MANUFACTURERS IN THIS REPORT DOES
NOT CONSTITUTE AN OFFICIAL INDORSEMENT OR APPROVAL OF
THE USE OF SUCH COMMERCIAL HARDWARE OR SOFTWARE.**

REPORT DOCUMENTATION PAGE		READ INSTRUCTIONS BEFORE COMPLETING FORM
1. REPORT NUMBER TR-RL-81-2 ✓	2. GOVT ACCESSION NO. AD-A097299	3. RECIPIENT'S CATALOG NUMBER
4. TITLE (and Subtitle) Acoustical Holographic Recording with Coherent Optical Readout and Image Processing		5. TYPE OF REPORT & PERIOD COVERED Technical Report
		6. PERFORMING ORG. REPORT NUMBER
7. AUTHOR(s) Hua-Kuang Liu		8. CONTRACT OR GRANT NUMBER(s) DA1162303A214
9. PERFORMING ORGANIZATION NAME AND ADDRESS Commander US Army Missile Command ATTN: DRSMI-RL Redstone Arsenal, Alabama 35898		10. PROGRAM ELEMENT, PROJECT, TASK AREA & WORK UNIT NUMBERS AMCMS 6123032140911
11. CONTROLLING OFFICE NAME AND ADDRESS Commander US Army Missile Command ATTN: DRSMI-RPT Redstone Arsenal, Alabama 35898		12. REPORT DATE 3 OCTOBER 1980
13. MONITORING AGENCY NAME & ADDRESS (if different from Controlling Office)		13. NUMBER OF PAGES
		15. SECURITY CLASS. (of this report) Unclassified
		15a. DECLASSIFICATION/DOWNGRADING SCHEDULE
16. DISTRIBUTION STATEMENT (of this Report) Approved for public release; distribution unlimited.		
17. DISTRIBUTION STATEMENT (of the abstract entered in Block 20, if different from Report)		
18. SUPPLEMENTARY NOTES This work was accomplished through the Laboratory Research Cooperative Program (LRCP) between Dr. Hua-Kuang Liu of the University of Alabama and the US Army Missile Command.		
19. KEY WORDS (Continue on reverse side if necessary and identify by block number) Acoustical Holography Acoustical Speckle Interferometry Acoustical Interferometry Flow-Detection and Quantification		
20. ABSTRACT (Continue on reverse side if necessary and identify by block number) New acoustic holographic wave memory devices have been designed for real-time in-situ recording applications. The basic operating principles of these devices and experimental results through the use of some of the proto-types of the devices are presented. Recording media used in the device include thermoplastic resin, Crisco vegetable oil, and Wilson corn oil. In addition, nonlinear coherent optical image processing techniques including equidensitometry, A-D conversion, and pseudo-color, all based on the new contact screen technique, are discussed with regard to the enhancement of the normally poor-resolved acoustical holographic images.		

SECURITY CLASSIFICATION OF THIS PAGE(When Data Entered)



SECURITY CLASSIFICATION OF THIS PAGE(When Data Entered)

TABLE OF CONTENTS

	Page No.
I. Introduction	3
II. Acoustic Holographic Wave Memory Device (AWMD)	3
A. Device Design	3
B. Operating Principle of the AWMD	3
(1) Interaction of ultrasound with the liquified surface	3
(2) Optical reconstruction of the acoustical surface hologram	6
C. An Alternative Design of the Device -- Ultrasonic Grating Added AWMD (UGAWMD)	8
D. Experimental Results	10
(1) AWMD	10
(2) UGAWMD	10
III. Applications of New Coherent Optical Image Processing Techniques to the Reconstructed Acoustical Holographic Images	19
A. Equidensitometry	19
(1) The fabrication of the contact screens	19
(2) The production of high-order contours (or equidensitometry)	20
B. Analog-to-Digital Conversion	23
C. Pseudo-color	23
IV. Conclusion	27
References	28
Distribution	29

Accession For	
NTIS CPAD	<input checked="" type="checkbox"/>
ERIC	<input type="checkbox"/>
USCIB	<input type="checkbox"/>
Justification	
By	
Date	
Availability Codes	
Available and/or	
Dist	Special
A	

LIST OF FIGURES

Figure No.		Page No.
1	Lower part of a type of AWMD.	1
2	Upper part of a type of AWMD.	2
3	The acoustical holographic recording system with in-situ real-time optical image reconstruction.	7
4	UGAWMD with a one-dimensional ultrasonic grating element.	9
5	Acoustical holographic and coherent optical image detection system.	11
6	Test object: metal washer and tapes mounted on a plastic board.	12
7	The optical image of the S-25 thermoplastic AWMD surface without the application of any acoustic waves.	13
8	(a) Optical display of the acoustic image by the S-25 AWMD and	14
	(b) The same image after the acoustic waves were turned off.	14
9	Optical image of the in-line water surface hologram of the test object as shown in Figure 6.	15
10	(a) UGAWMD with window screen as diffraction gratings.	16
	(b) A close-up shot of a portion of the UGAWMD.	16
11	Holographic images of the test object as shown in Figure 6 by UGAWMD with object beam only.	
	(a) All orders are present	
	(b) Order is blocked. 50 μ m of water is used in UGAWMD.	17
12	Holographic images recorded by UGAWMD of	
	(a) The test object; a handle; and	18
	(b) The image with all orders present. 50 μ m of Wilson corn oil is used as the medium of UGAWMD.	18
13	A three level contact screen produced by one translation of a Ronchi Ruling mask and two exposures.	21
14	A coherent optical image processing system	22
15	Illustration of how three-bit outputs, I_{01} , I_{03} , and I_{07} , are generated by single contact screen photograph with eight different bar widths.	24
16	Intensity outputs I_{Bg} , I_{Gm} , and I_{Rn} versus b/a for $\ell = 1$, $m = 2$, and $n = 4$	26

ACOUSTICAL HOLOGRAPHIC RECORDING WITH COHERENT OPTICAL READOUT AND IMAGE PROCESSING

I. Introduction

The idea of applying thermoplastic material to the recording of acoustic holograms¹ has been recently investigated.²⁻⁴ It has been found that certain thermoplastic resins indeed have the capability of retention of acoustic images. This report will present further findings in real-time, in-situ thermoplastic recording and retention of acoustic holograms. A new acoustical wave recording device and its modified version are described in Section II. In the same Section, basic operation principles including optical image reconstruction of the device as well as experimental results are also presented. The modified device has a built-in two-dimensional ultrasonic diffraction grating similar in principle to the one-dimensional grid used previously.⁵

For image enhancement of the acoustic holograms, a few new coherent optical image processing techniques are discussed in Section III. The new techniques are based on new contact screens.⁶⁻⁷ These techniques include equidensitometry, A-D conversion, and pseudo-color. Section IV is the conclusion which discusses the merit of the device, limitations of the system and recommends further work.

II. Acoustic Holographic Wave Memory Device (AWMD)

A new acoustical wave recording device was designed. The device can be used in real-time to record and retain acoustical waves; their interference patterns, or the acoustical holographic images in an acoustical imaging system.

A. Device Design

The essential parts of the device can be illustrated with an example described below.

In Figure 1, *A* is a thin piece of supporting material that, ideally, should be almost transparent to acoustical waves, e.g., a thin piece of plexiglas. The purpose of part *B* is to enclose an area so that a uniform layer of thermoplastic resin (such as S-25, Foral 85, Foral 105, staybelite Ester 10 of Hercules Inc., Wilmington, Delaware, U.S.A.), or any other material can be softened from its originally hardened state by elevating its temperature.

In Figure 2, *C* is a piece of quartz, or thermally treated glass, or any piece of optically transparent material that is coated by a thin uniform layer of electric resistive material such as indium oxide (InO) or tin oxide (SnO) as indicated by *D*. The thickness of *D*, usually around a few microns, determines the resistance of the material. At the two opposite ends of *C* along the *y*-direction, electrodes *E* are fixed and in contact to *D* so that a.c. or d.c. electric energy can be applied to generate heat in *D*.

The finished AWMD is made by combining the parts in Figures 1 and 2 in the following manner:

Placing the part in Figure 1 horizontally with the thermoplastic layer facing up and covering it with the part shown in Figure 2 with the electric resistive material facing down toward the thermoplastic material of Figure 1. The *x*- and *y*-directions of Figures 1 and 2 should be aligned with each other respectively and the whole area of the thermoplastic material should be closely covered. The edges should be totally sealed so that liquid cannot leak into the device.

B. Operating Principle of the AWMD

(1) Interaction of ultrasound with the liquified surface.

In the acoustical holographic system shown in Figure 3, a reference beam of amplitude A_r , generated by the reference transducer, is incident upon the surface ($z=0$) of the thermoplastic layer at an angle ϕ_r , while the object beam with amplitude A_{ob} is incident at any angle θ_o with respect to the perpendicular to the surface and carries an object-dependent phase $\theta(x,y)$. If the object is simple, such as a coarse grating structure, part of the beam generated by the object transducer may propagate through the object plane without being modulated by the object. The portion of the beam with amplitude A_o , and incidence angle ϕ_o , may be considered as a reference beam for the hologram. These waves are listed below:

$$\text{Reference beam No. 1: } R_1 = A_r \exp(jk_r y) \quad (1)$$

$$\text{Object beam: } O = A_{ob} \exp[j(k_o y + \theta(x,y))] \quad (2)$$

$$\text{Reference beam No. 2: } R_2 = A_o \exp(jk_o y) \quad (3)$$

where

$$k_r = \frac{2\pi}{\lambda} \sin \theta_r, \text{ and } k_o = \frac{2\pi}{\lambda} \sin \theta_o \quad (4)$$

and λ is the wavelength of the acoustic wave.

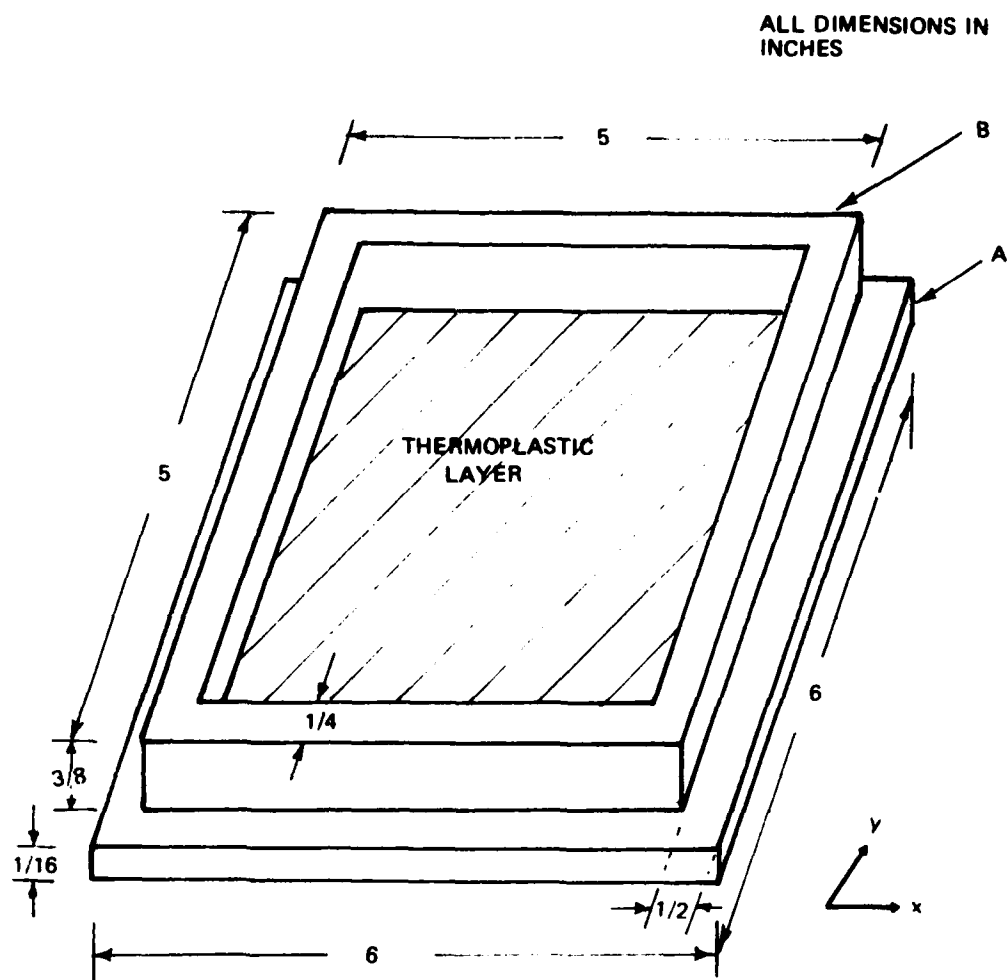


Figure 1. Lower part of a type of AWM

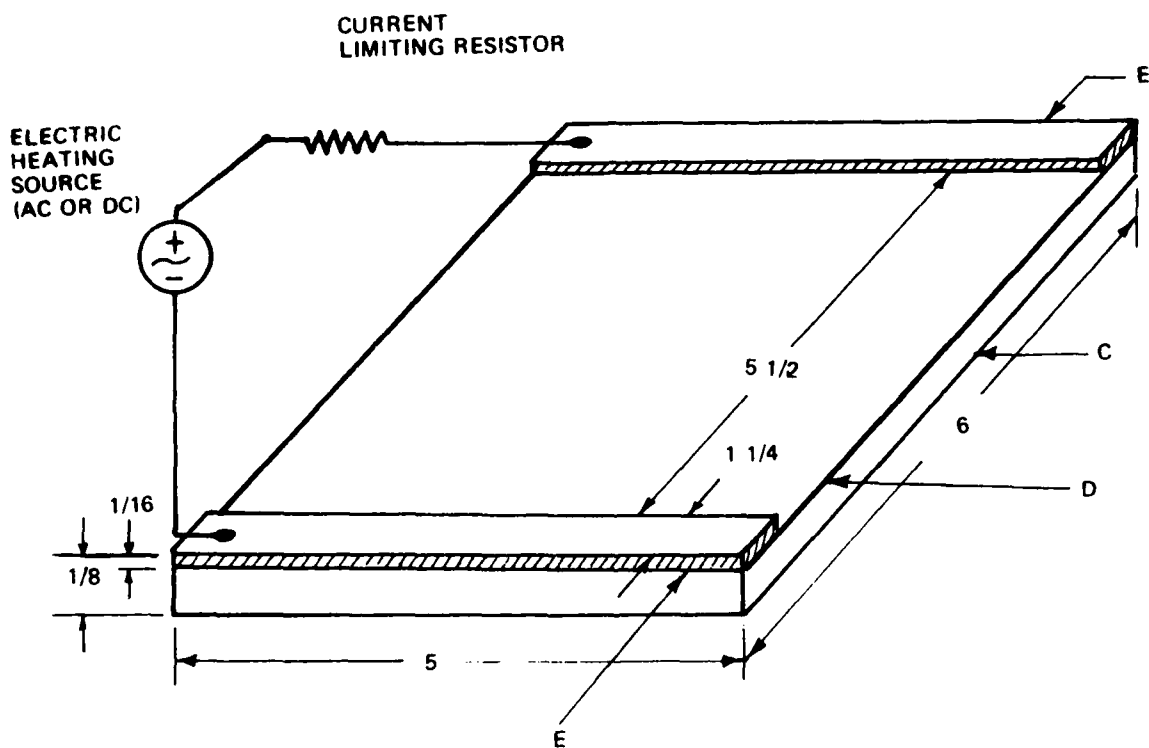


Figure 2. Upper part of a type of AWMD.

According to the derivations, under appropriate conditions, given in Reference 2, the ripple patterns of the liquid surface that is represented by z_s measured from the equilibrium plane ($z=0$) can be written as

$$z_s = 2\alpha \cos[(k_r + k_o)y + \phi] + 2\beta \cos[(k_r + k_o)y] + 2\gamma \cos \phi + \kappa \quad (5)$$

where,

$$\alpha = \frac{A_r A_o}{\rho V_s^2 [\rho g + c (k_r + k_o)^2]} \quad (6)$$

$$\beta = \frac{A_r A_o}{\rho V_s^2 [\rho g + c (k_r + k_o)^2]} \quad (7)$$

$$\gamma = \frac{A_r A_o}{(\rho^2 g V_s^2)} \quad (8)$$

$$\kappa = \frac{A_r^2 + A_o^2 + A_s^2}{(\rho^2 g V_s^2)} \quad (9)$$

In the above equations, ρ is the density of the recording material; V_s is the velocity of sound in the medium and g is the gravitational constant.

The physical meaning of equation (5) is described below. There is a bulge of height $2\gamma \cos \phi(x,y) + \kappa$ in the region where the acoustical wave is applied. Impressed upon this bulge are two interference patterns with the same spatial wave number, $k_r + k_o$, but different amplitudes 2α and 2β . One of the patterns is different from the other by a phase $\phi(x,y)$. If the amplitude of the reference beam Number 1 is set equal to zero, then from Eqs. (6) and (7) we find $\alpha=\beta=0$ and $\kappa = (A_{ob}^2 + A_o^2)/(\rho^2 g V_s^2)$. The bulge is slightly reduced in height, and the interference patterns still exist. The object geometry still modifies the liquefied surface, in a similar way as in the case of an in-line hologram. On the other hand, if the amplitude of the reference beam Number 2 is zero, Eq. (5) becomes

$$z_s = 2\alpha \cos[(k_r + k_o)y + \phi] + \kappa' \quad (10)$$

where

$$\kappa' = (A_r^2 + A_o^2)/(\rho^2 g V_s^2) \quad (11)$$

Equation (10) represents the interference pattern resulting from a typical off-axis hologram.

(2) Optical Reconstruction of Acoustical Surface Hologram

The detection of the acoustical hologram can be achieved by the technique of coherent optical image reconstruction. Assume that a laser beam plane wave of amplitude A_q and wavelength Λ is normally incident (oblique incidence is also possible with additional complication in the mathematical manipulations) on the surface where the acoustical hologram is recorded. The light beam is expressed by

$$s(z) = A_q e^{j \frac{2\pi}{\Lambda} z} + A_q e^{-j \kappa_q z} \quad (12)$$

where $\kappa_q = \frac{2\pi}{\Lambda}$ is the wave number of the light wave.

After reflection from the surface hologram, the amplitude $s(z)$ is multiplied by a factor R and the phase of the beam is modified by the added term $2z_s(x,y)$, where $z_s(x,y)$ is in general given by Eq. (5). The reflected light beam may then be written as

$$S_r(x,y) = R e^{j \kappa_q (z + 2z_s)} \left\{ [1 + j 2[(\alpha \kappa_q + \beta \kappa_q) e^{j(k_r + k_o)y} + \gamma \kappa_q] e^{j\phi}] + j 2[(\alpha \kappa_q + \beta \kappa_q) e^{j(k_r + k_o)y} + \gamma \kappa_q] e^{j\phi} \right\} \quad (13)$$

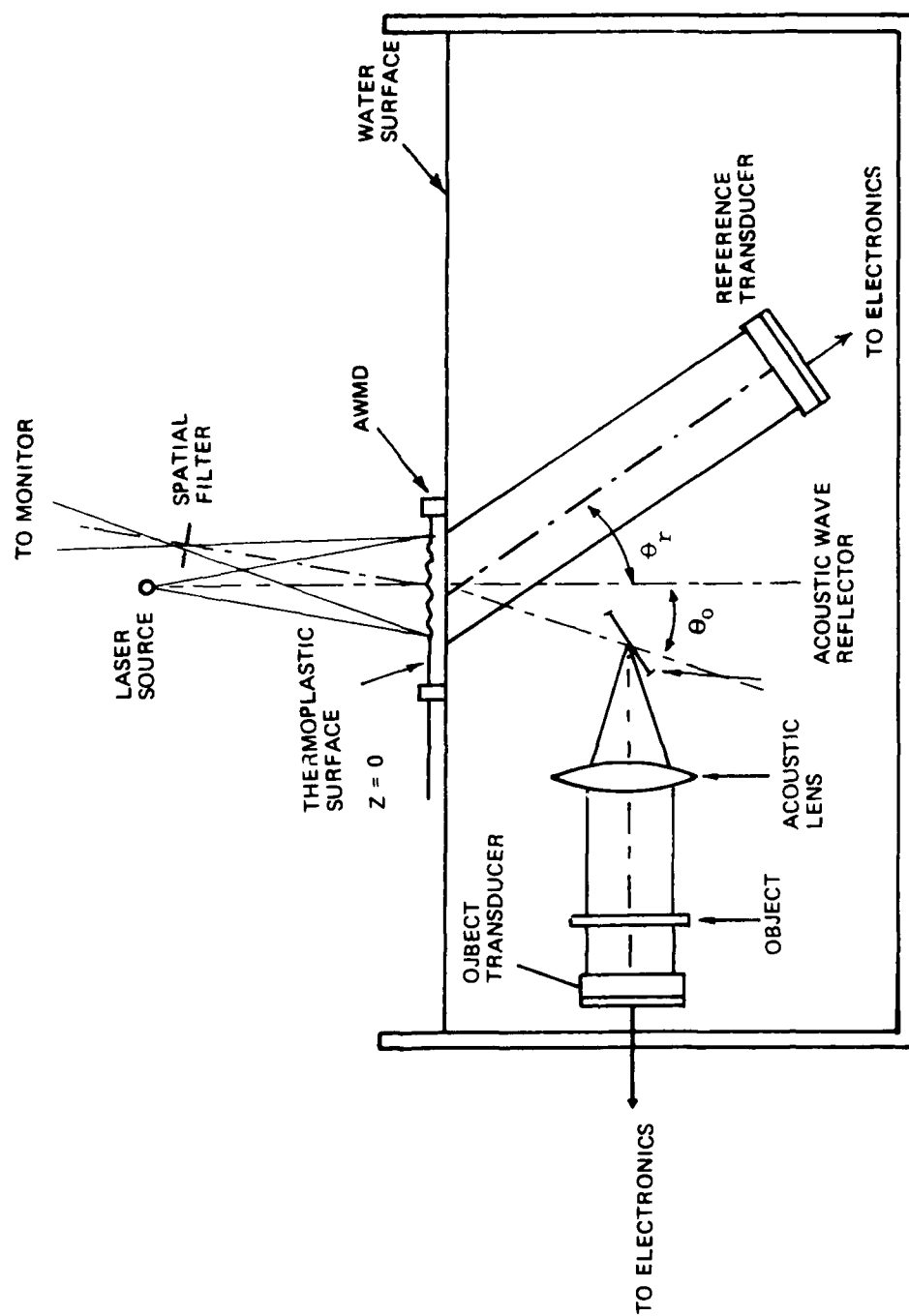


Figure 3. The acoustical holographic recording system with in-situ real-time optical image reconstruction.

The important part of Eq. (13) for the optical image reconstruction is the positive first order diffraction term, or the term that contains $e^{j\phi}$. The phase term is identical to that of the object beam given by Eq. (2), and the amplitude A_{ob} of the original object beam is also contained in α and γ . The following two special cases are considered:

Case 1:

$A_o = 0$, so that $\beta = 0$, $\gamma = 0$.

$$S_{r1}(x,y) = j2R e^{jk_g(z+2\kappa)} \left[\alpha k_g e^{j(k_x + k_o)y} \right] e^{-j\phi} \quad (14)$$

A spatial filter can be placed in the Fourier plane and the term $S_{r1}(z,y)$ can be isolated for the holographic image reconstruction.

Case 2:

$A_o = 0$ but $A_r \neq 0$, this implies $\alpha = \beta = 0$, hence

$$S_r(x,y) = j2R \gamma k_g e^{jk_g(z+2\kappa)} e^{-j\phi} \quad (15)$$

The amplitude and phase of the object beam is still contained in $S_r(x,y)$.

Therefore the image of the in-line acoustical hologram can also be optically reconstructed by the proper spatial filtering process.

C. An Alternative Design of the Device - Ultrasonic Grating Added AWMD (UGAWMD).

The in-line holographic images obtainable in the AWMD as described previously has a basic and serious drawback, i.e., the conversion of the optical phase variations into intensity variations do not adequately reproduce the low spatial frequency part of the image. This is the reason that an angularly-offset acoustic reference beam is used in the system. The function of the reference beam is to make the image information (including the low spatial frequency portion) be modulated onto a high-spatial-frequency carrier.

The requirement of the additional ultrasonic reference beam, however, add other limitations to the system. The reference beam must be in coherence with the object beam; the reference beam must be uniform over the device recording area, and finally, because of the necessity of the maintenance of a correct angle between the object and the reference beams, the positions of the lenses and object under test are restricted.

Fortunately, another method can be used to modulate the image information into a high-frequency spatial carrier. Either a one-dimensional or a two-dimensional ultrasonic grating can be placed beneath the AWMD. We shall call the modified structure UGAWMD. An example of the UGAWMD with a one-dimensional grating consisting of alternative strips of transmissive and attenuative material is illustrated in Figure 4. When the UGAWMD is used to replace the AWMD in the acoustical holographic system, the reference beam transducer can be removed from the system.

In general, the acoustic amplitude transmission function of a two-dimensional periodic grating structure of opaque bars of width d and periods W along the x - and y -direction can be written as

$$T(x,y) = \left\{ \text{rect}\left(\frac{x}{W-d}\right) * \left[\sum_{n=-\infty}^{\infty} \delta(x-nW) \right] \right\} \cdot \left\{ \text{rect}\left(\frac{y}{W-d}\right) * \left[\sum_{n=-\infty}^{\infty} \delta(y-nW) \right] \right\} \quad (16)$$

where

$$\text{rect}(x) = \begin{cases} 1, & |x| \leq 1/2 \\ 0, & |x| > 1/2 \end{cases} \quad (17)$$

and

$$\delta(x) = \begin{cases} 1, & x = 0 \\ 0, & x \neq 0 \end{cases} \quad (18)$$

The radiation pressure of the acoustic waves caused by the object transducer alone is given by

$$p(x,y) = T(x,y) |O+R_2|^2 / (\rho V_s^2), \quad (19)$$

where ρ is the density of the thermoplastic or any other recording material and V_s is the velocity of sound.

Substituting O and R_2 from Eqs. (1) and (2) into Eq. (19), the radiation pressure of the wave incident at the liquid surface becomes

$$p(x,y) = \frac{1}{\rho V_s^2} [A_{ob}^2 + A_{oi}^2 + 2A_{ob}A_{oi} \cos \phi(x,y)] \quad (20)$$

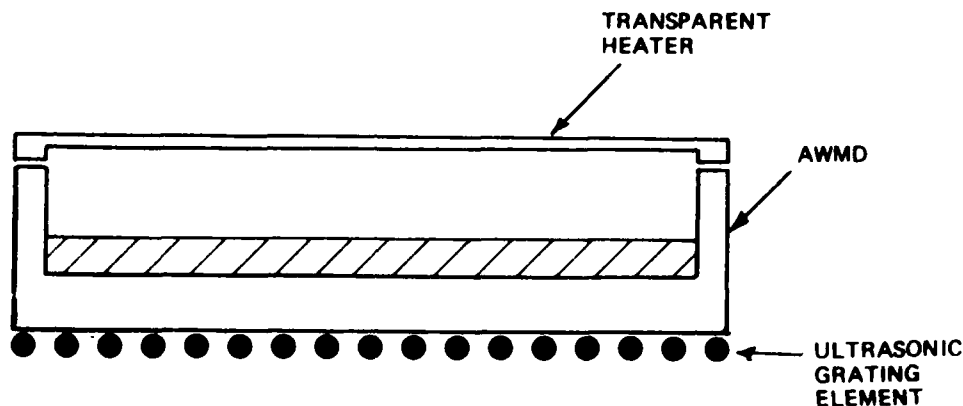


Figure 4. UGAWMD with a one-dimensional ultrasonic grating element.

The solution for the ripple pattern becomes much more complicated because of the additional term $T(x,y)$ in Eq. (20). However, an assumption can be made to obtain some physical insight to this problem. It is assumed that the grating pattern is approximately reproduced on the liquid surface. Then the pattern at the Fourier plane of the optical imaging lens is the Fourier transform of the diffraction grating pattern convolving with the image ripple pattern of the object under test. For example, in case that the reference beam is zero, part of the object image pattern has been previously described by Eq. (15). The Fourier transform of Eq. (16) can be written as

$$\begin{aligned} [T(x,y)] = & \left[\sum_{n=-\infty}^{\infty} \delta \left(\frac{x}{\Delta f} - \frac{n}{W} \right) \right. \\ & \left. \frac{1}{j\Delta f} \exp(jkf) \exp \left[\frac{k}{j2f} x_1^2 \right] (W-d) \operatorname{sinc} \left[\frac{(W-d)x_1}{\Delta f} \right] \right] \\ & \left[\sum_{n=-\infty}^{\infty} \delta \left(\frac{x}{\Delta f} - \frac{n}{W} \right) \right] \frac{1}{j\Delta f} \exp(jkf) \exp \left[\frac{k}{j2f} y_1^2 \right] \\ & (W-d) \operatorname{sinc} \left[\frac{(W-d)y_1}{\Delta f} \right] \}. \end{aligned} \quad (21)$$

when n is an integer, f is the focal length of the Fourier imaging lens, x_F and y_F denotes the Cartesian coordinates at the Fourier plane. After the convolution operation the intensity of the n -th order diffraction terms centered at

$$x_i = \frac{n\lambda f}{W}, \quad \text{and} \quad (22)$$

$$y_i = \frac{n\lambda f}{W}, \quad (23)$$

will be proportional to the object image pattern and the term $n^{-2} \sin^2 [n\pi(1 - \frac{d}{W})]$. Obviously, the most important contribution is due to the first order term where $n = \pm 1$ since the second order term will have $\frac{1}{4}$ the value of the first order term.

The advantage of the diffracting effect of the acoustical gratings is offset by the fact that the gratings will unavoidably reduce the total acoustical energy for the creation of the image recording on the liquid surface. Nevertheless, the simplification of the system as a result of the omission of the object beam transducer makes the UGAWMD a much improved device for the acoustical imaging system.

D. Experimental Results

Various objects are being tested in the acoustic holographic system as shown in Figure 5.

Experimental results have been obtained both for the regular AWMD and the UGAWMD. These results are presented as follows:

(1) AWMD:

Recordings by AWMD of a metal washer and stripes of tapes arranged in triangular form and mounted on a plastic board is shown in Figure 6. As shown in the figure, the length of each of the tapes is approximately 2 inches. Thermoplastic S-25 with softening temperature of 25°C is used in the AWMD. The optical image of the recording area of the device is shown in Figure 7. Positioning of the device and the fabrication of the device are not optimized. The recordings of the image of the test object of Figure 6 by the S-25 AWMD at 20°C and without any heating is detected optically and shown in Figure 8(a). It is worthwhile to mention that the reference beam is not used and spatial filtering at the Fourier plane of the optical lens is not performed when this photograph is taken. The capability of the retention of the image is shown in Figure 8(b); the image is still visible 2 minutes after the turning-off of the acoustic waves. For comparison, the optical image of the water surface in-line hologram of the same test object is shown in Fig. 9. It has been observed that the water surface hologram has little stability and has no memory capability at all.

(2) UGAWMD:

An example of the UGAWMD discussed previously is realized by attaching a window screen beneath the AWMD. The actual dimension and the details of a corner of the UGAWMD are shown in Fig. 10. The spatial frequency of the 2-dimensional grating is approximately 1.25 cm^{-1} .

The UGAWMD is first filled with water to an approximate thickness of $50\mu\text{m}$. The reference beam is turned off while the optical reconstruction of the acoustic image is recorded. The image with all orders present is shown in Fig. 11(a). When the zero-order is blocked, the image is shown in Fig. 11(b). The speckle patterns of Fig. 11(a) are due to the ultrasonic grating which in this case is the window screen.

For the purpose of exploring the possibility of using other recording media, Crisco cooking oil and Wilson corn oil have been used in the UGAWMD. Crisco oil freezes at room temperature. It has the possibility of making a permanent recording although this has not been observed in the laboratory up to date. Nevertheless, it has been proved that recording of holographic images can be done when it is in the liquified state. Also, it has been found that Wilson corn oil seems to be a better recording material than water in making recordings in UGAWMD. A handle as shown in Fig. 12(a) is used as the test object. Optical image reconstruction of the acoustical hologram is shown in Fig. 12(b). It can be seen that the caved-in portion of the plastic handle appeared to be brighter in the image. A $50\mu\text{m}$ Wilson oil is used in the UGAWMD. It can be seen that the diffraction gratings are imaged much more clearly when the oil is used than in the case when water is used.

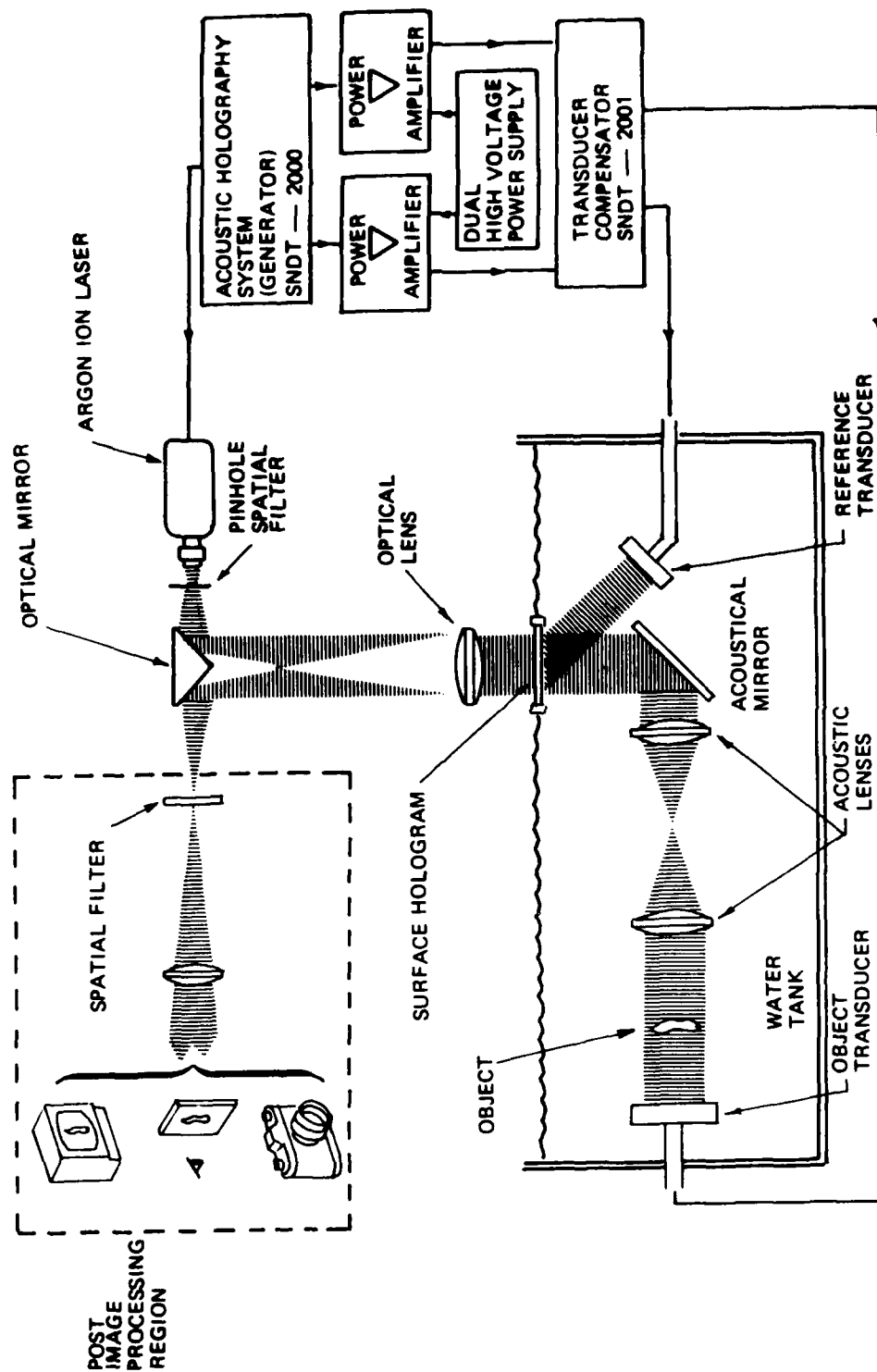


Figure 5. Acoustical holographic and coherent optical image detection system.

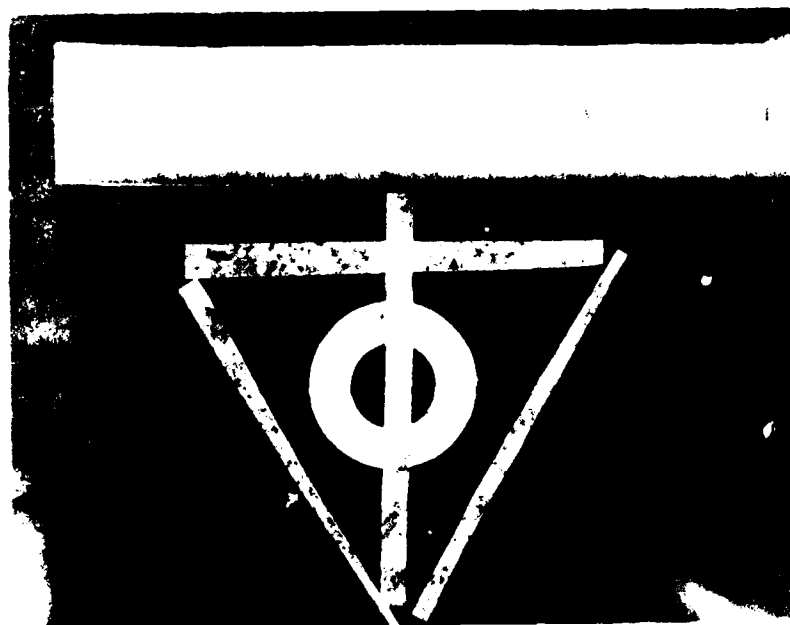


Figure 6. Test object: metal washer and nut on corner of a plastic board.

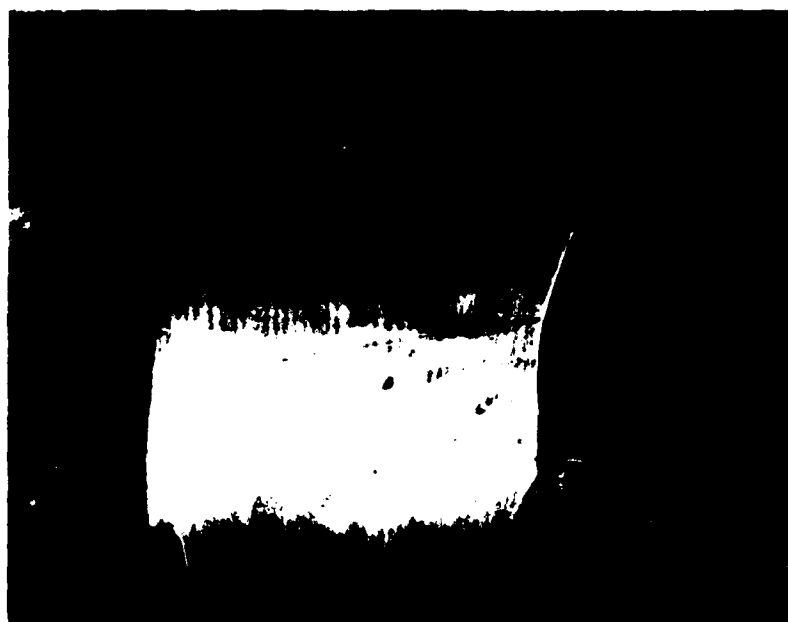
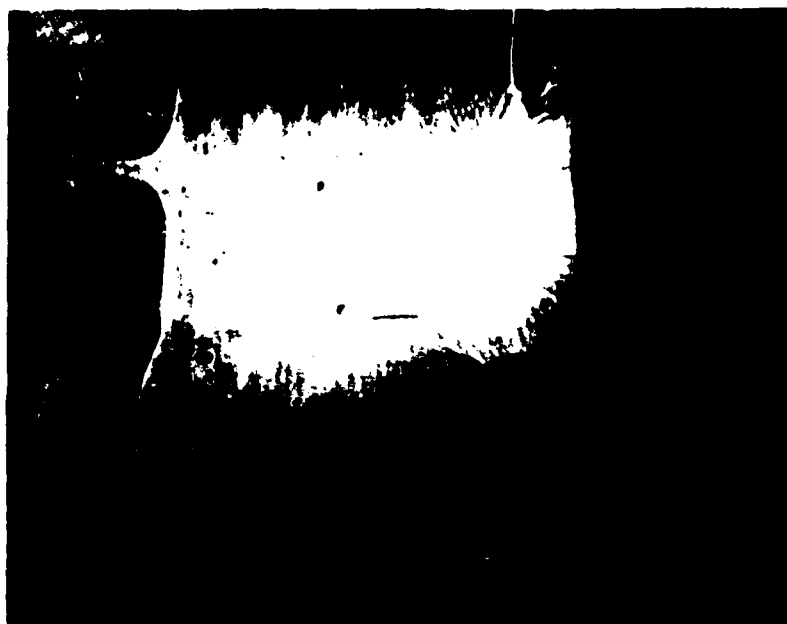


Figure 1. Optical image of the S-28 thermoplastic AWB's at 100x magnification. The scale bar is 100 μ m.



64

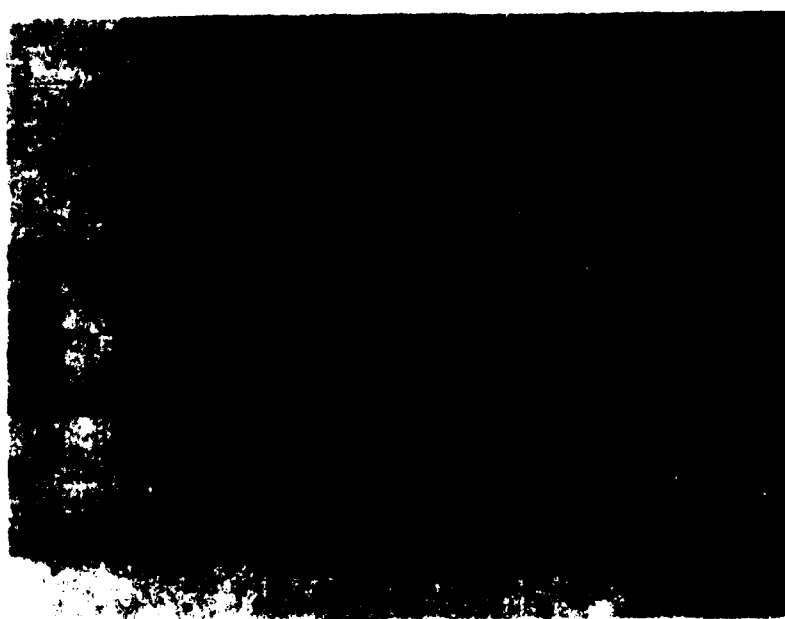
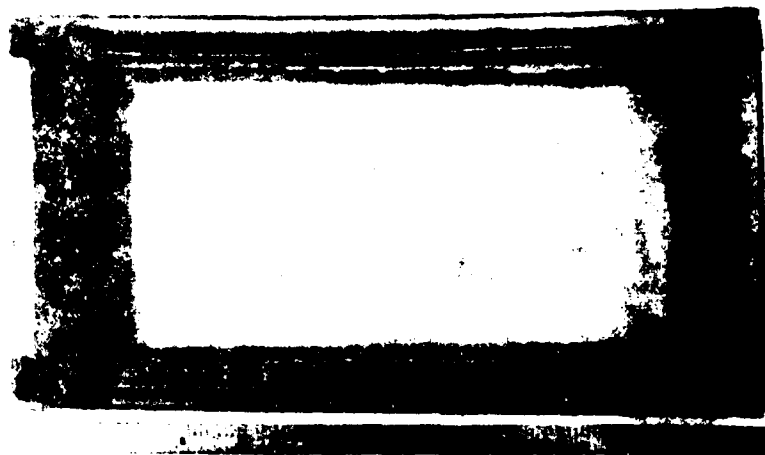


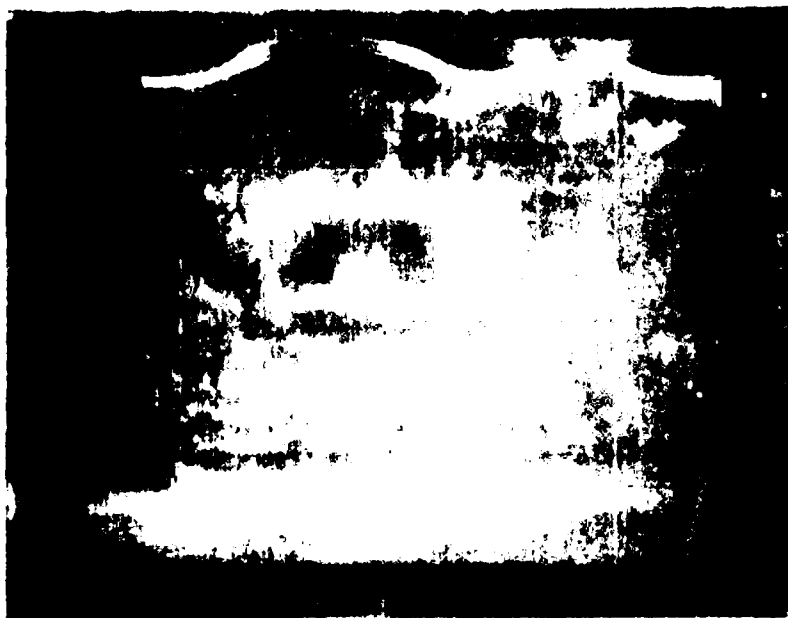
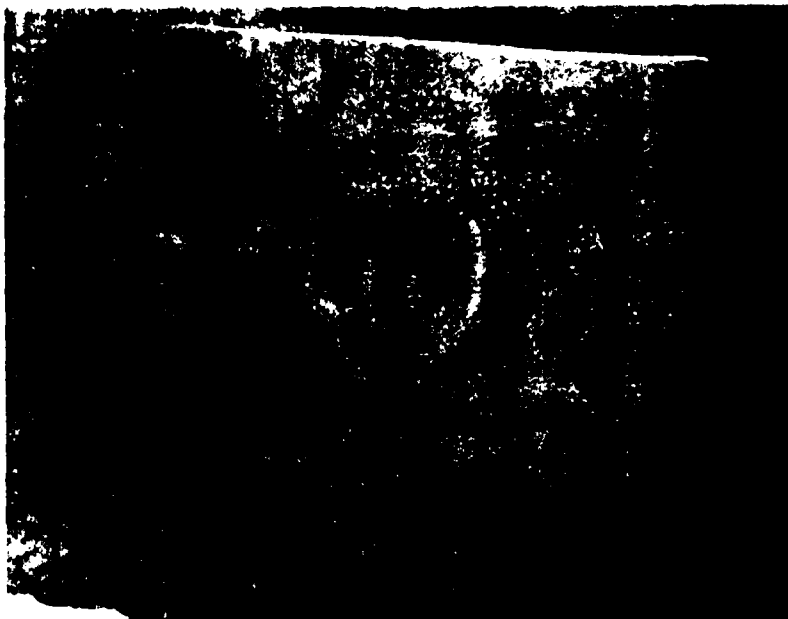
65

64. Close-up of the debris from the N. 7. BWD and
65. The same image after the debris has been washed out.

[illegible]

• *sublimation*



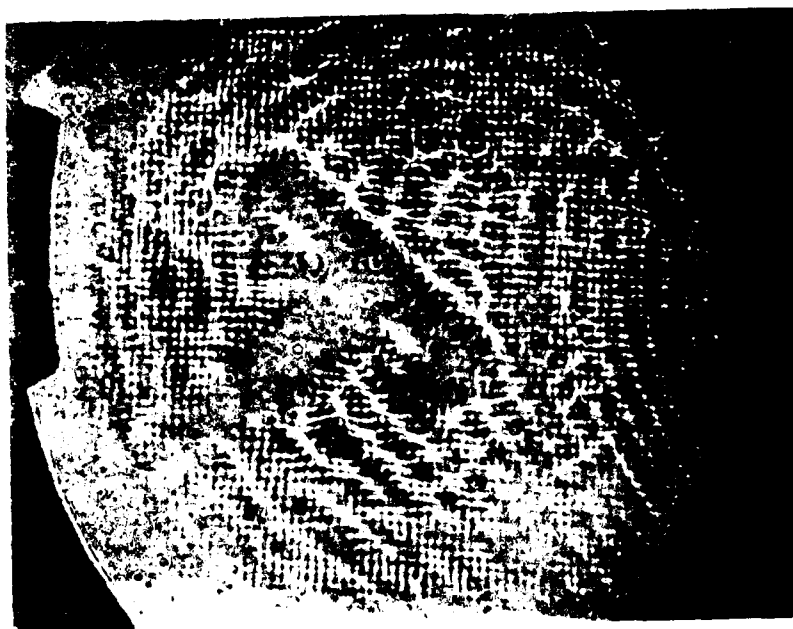


100-100000

100-100000



100



44

$$H^0(\mathcal{O}_X) = H^0(X, \mathcal{O}_X) = H^0(X, \mathbb{C}) = \mathbb{C}.$$

1. *How much time do you spend on the Internet each week?*
 2. *How much time do you spend on the Internet each day?*

$\mathcal{G} = \text{Aut}(W)$ and $\mathcal{H} = \text{Aut}(W)$ are the automorphism groups of W and W respectively.

III. Applications of New Coherent Optical Image Processing Techniques to the Reconstructed Acoustical Holographic Images

One main problem of acoustical holography is the poor resolution of the reconstructed image. Although electronic scanning methods have gained high signal-to-noise ratios in image reconstruction, the time required to scan over the total image area makes the method impractical especially in the detection of a moving object. The acoustical images recorded by the AWMD and UGAWMD as shown in the previous section have demonstrated the need for better spatial filtering arrangement.

Spatial filtering schemes can be applied in the post image processing region as enclosed by dotted lines in Fig. 5. Optical filters such as stops and phase retarders can be inserted in the focal plane of the imaging lens. Both linear and quadratic phase-contrast modes of optical filters can be used. The linear mode can produce images of greater brightness; the quadratic mode, on the other hand, can make the grid structure *less distinctive to the eye*.

Electronic digital signal processing techniques can also be applied for the image enhancement of the optically reconstructed image. However, the sequential processing method is time consuming. This drawback often offsets its merit of high flexibility.

In this Section, a few new methods of optical filtering based on contact screens will be discussed. These methods should be useful for the image enhancement, and suppression of noise in acoustical holographic images. The methods include equidensitometry, A-D conversion, and pseudo-color by coherent optical filtering. All of the methods utilize the non-linearity generated by the use of the contact screens. A detailed description is given below.

A. Equidensitometry

The contact screen technique, similar to that which is being widely used in the printing industry, has recently proved to be useful in achieving monotonic and non-monotonic nonlinear characteristics in a coherent optical data processing system. In the printing industry two-dimensional halftone commercial screens are used. The screen has a closely packed matrix of small dots, each with a pre-determined density profile. However, for nonlinear optical data processing applications, only one-dimensional halftone screens, or periodic line structures are needed. A special simple example of these screens is the Ronchi ruling, which has periodic equal-width opaque straight bars imprinted on a transparent glass plate. The spacing between any two bars is of the same width as the opaque bar.

A fundamental difficulty in the nonlinear optical data processing work is the design and fabrication of the halftone screens. A new and simple method for the fabrication of multilevel contact screens is described herein as well as the way they are used in achieving equidensitometry, optical A-D conversion and pseudo-color.

(1) The fabrication of the contact screens

The following two approaches can be used to fabricate a contact screen.

(i) Assume that there is available a one-dimensional mask which has a periodic intensity transmittance function $T(x)$ of period a , i.e., $T(x) = T(x+a)$, and

$$T(x) = \begin{cases} 1 & 0 < x \leq a/N \\ 0 & a/N < x \leq a \end{cases} \quad (24)$$

where $N \geq 2$.

In the making of the contact screen, a low- γ negative film is placed below, and in close contact with, the mask. The film can be made to traverse along the x -direction by means of a translation stage while the mask is fixed. At an initial position of the film, the mask and film are exposed by a uniform incoherent light source for a time τ_1 . After the exposure the film is translated along the x -direction for a distance a/N . A second exposure of duration τ_2 is made. The process of stepping a distance a/N and exposing for a time τ_i goes on until the $(n-1)^{th}$ translation and N^{th} exposure are completed. The spatial distribution of exposure becomes

$$E(x) = p \tau_i \quad (i-1)a/N \leq x < i a/N \quad (25)$$

where $i = 1, 2, \dots, N$, and p is the local average light power per unit area. If $E(x)$ is located in the linear region of the Hurter-Driffeld (H&D) curve, the developed film will have a density distribution $D(x)$ expressed as

$$D(x) = \gamma \log E(x) - D_0 \quad (26)$$

where γ is the slope of the linear region of the curve, and $-D_0$ is the extrapolated value of density where the straight-line approximation would meet the D -axis. On the other hand, if some of $E(x)$ were in the non-linear region of the H&D curve of the film, Eq. (26) can no longer be applied over the whole range. In this latter case, a pre-calibration of the exposures can be used assure that the desired density levels are achieved. The advantage of the approach described above is that various values of τ_i can be used to shape the periodic density distribution of the contact screen to any predetermined form.

(ii) If the original one-dimensional periodic mask has an intensity transmittance function $T(x)$, like that of a Ronchi ruling shown in Fig. 13(a), it can be described by Eq. (24) with $N = 2$. A different translation-exposure pro-

cess can now be used in order to obtain a multi-level contact screen. An example is given in Fig. 13, where a three level screen is generated. With the Ronchi ruling placed in close contact with an Agfa 10E56 photographic plate, a first exposure by an incoherent light source is made. Then the plate is translated an amount $\Delta x = a/3$, and a second exposure is made. After the photographic plate is developed, its density profile will be as shown in Fig. 13(c). The three levels of density are $D = D_0$ (fog level), D_1 and D_2 . The density profile can be described as

$$\begin{aligned} D(x) &= D(x+a) & , & \text{and} \\ D(x) &= D_1 & , & 0 < x \leq a/6 \text{ and} \\ & & & a/2 < x \leq 2a/3 , \\ &= D_2 & , & a/6 < x \leq a/2 , \\ &= D_0 & , & 2a/3 < x \leq a . \end{aligned} \quad (27)$$

The densities D_1 and D_2 are dependent on the exposure and development times used. Even if the exposure times are equal and the exposure is in the linear region, $D_2 \neq 2D_1$ in general, due to the term D_0 in Eq. (26). Hence D_1 and D_2 can only be determined either by pre-calibration or by microdensitometer measurement after the fact. The method can be extended to fabricate an N-level screen simply by translating the film plate (N-2) times through a distance a/N for each (N-1) exposure. The density profile of the developed film may be controlled by the exposure times involved.

Both of the approaches described above require relatively unsophisticated equipment. The step size of the screen is controlled by the accuracy of the translation stage.

(2) The production of high-order contours (or equidensitometry)

(i) Principle of contact screen photograph fabrication.

In the application of the contact screen method to produce contours of constant brightness on a continuous tone photograph, the first step is to produce a contact screen photograph of the original object. This can be done by simply contact printing the original photograph or photographic image (such as the acoustic holographic image) through the contact screen on a high- γ (high contrast) copying film. The exposure of the film for a time interval τ produces an exposure defined by

$$E(x,y) = p \cdot \tau [D(x) \cdot D_p(x,y)] , \quad (28)$$

where $D(x)$ and $D_p(x,y)$ are the density distributions of the contact screen and the continuous tone image, respectively.

The copying film has a threshold level E_t such that after the development of the exposed film the transmittance of the film will be a binary-type function. Assuming that the γ of the film is very large, the transmittance of film may be written as

$$\begin{aligned} T(x,y) &= 1 , & E(x,y) < E_t , \\ &= 0 , & E(x,y) \geq E_t . \end{aligned} \quad (29)$$

The above equation indicates that the original continuous-tone photograph (or image) is converted to a spatially modulated binary photograph. The modulated photograph of the original object is called the contact screen photograph.

By control of the exposure level, $p \cdot \tau$ in Eq. (28), a variety of mappings of picture density into halftone line widths can be achieved. The maximum number of different widths in any contact screen photograph can not be greater than the number of gray levels of the contact screen.

(ii) Principle of contour generation

The contact screen photograph is placed in the input plane of a coherent optical data processing system, as shown in Fig. 14. The laser light is first spatially filtered by a conventional pin-hole spatial filter, and collimated by the lens, L_1 . The contact screen photograph is placed at the object plane of the lens, L_2 , and a multitude of diffraction orders from the quasi-periodic input appear in the focal plane. Any particular order of diffraction can be singled out at the Fourier plane of the lens L_2 by a translatable thin slit spatial filter. The output is then re-transformed by lens L_3 , producing a filtered image in its focal plane.

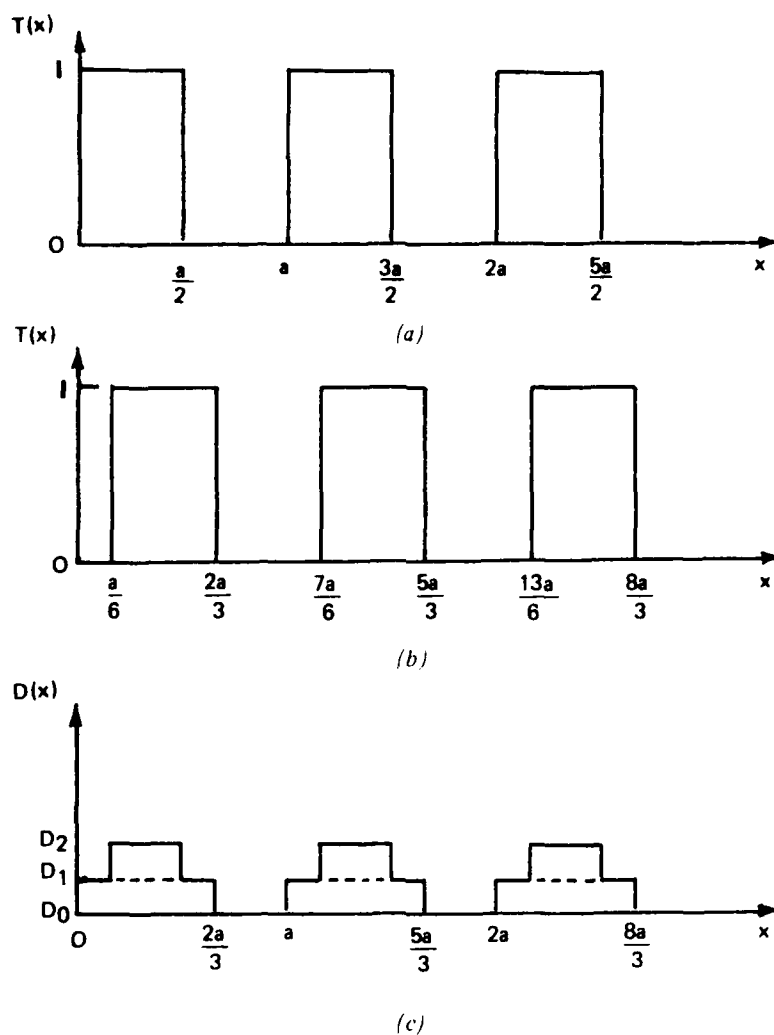


Figure 13. A three level contact screen produced by one translation of a Ronchi Ruling mask and two exposures.
 (a) Ronchi Ruling transmittance function with no translation. The period is a . A first exposure is made at this position.
 (b) Ronchi Ruling transmittance with a translation of the film plate of $\Delta x = a/3$. A second exposure is made at this position.
 (c) Density function of the resulted contact screen due to the exposures through the Ronchi Ruling.

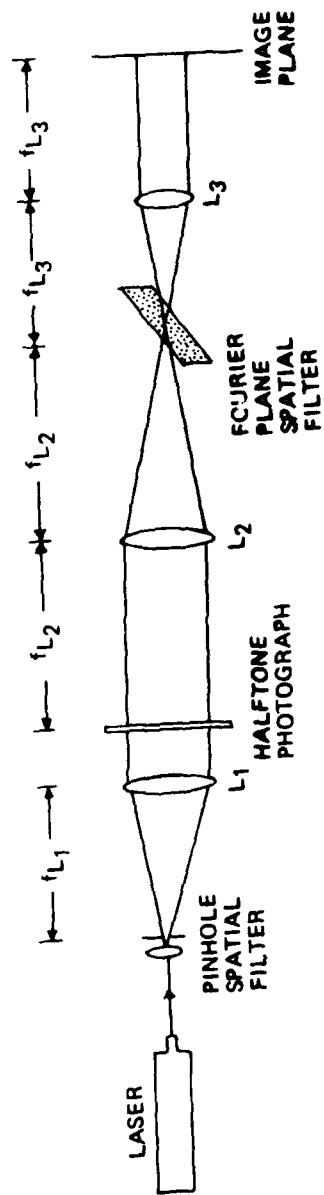


Figure 14. A coherent optical image processing system.

If the wavelength and geometrical factors are omitted for clarity, the n^{th} -order output intensity at the Fourier plane is

$$I_n(b/a) = \left(\frac{1}{n\pi} \sin n\pi b/a \right)^2 \quad (30)$$

and the normalized n^{th} order output may be written as

$$I_n(b/a) = n^2 \pi^2 I_n(b/a) = \sin^2 n\pi b/a \quad (31)$$

where $n \geq 1$ and b is the width of the opaque lines $b/a \leq 1$. The zero order output may be written as

$$I_0 = (1 - b/a)^2 \quad (32)$$

Equations (30)–(32) are derived using the assumption that an infinite number of periodic opaque lines of width b and period a are in the object plane. In reality, if a sufficiently large number of the opaque lines exists in a certain area, these equations may be considered as good approximations so that no aliasing phenomenon should prevail.

B. Analog-to-Digital Conversion

The principle of optical A-D conversion can be demonstrated as possible by using three different orders of a single contact screen, provided the three output images fall upon hard-clipping detectors.

Consider a periodic halftone screen of period a and intensity transmittance

$$T(x) = \begin{cases} 0, & 0 < x \leq a/2, \\ T_n \frac{a}{2} + \frac{(n-1)a}{14} < x \leq \frac{a}{2} + \frac{na}{14} \end{cases} \quad (33)$$

where $n = 1, 2, \dots, 7$, T_n are positive constants less than 1, and $T_m < T_n$ if $m < n$.

This contact screen can be used in the system to perform analog-to-digital conversion when the first, third, and seventh order outputs are used. Eight levels of digitization (3 bits) can be achieved. This example can easily be illustrated with the help of Fig. 15, where the normalized outputs I_1 , I_3 , and I_7 as described in Eq. (31) are plotted for $1/2 \leq b/a \leq 1$. The level I_{th} is the hard-clipping detection threshold which is common to the three normalized outputs, where the halftone bar width are marked. This threshold is naturally different for the corresponding unnormalized outputs, I_n , given in Eq. (30). The scheme is to set the output bits I_{01} , I_{02} , and I_{03} , respectively to 1 if $I_1 \geq (1/\pi^2)I_{th}$, $I_3 \geq (1/9\pi^2)I_{th}$, and $I_7 \geq (1/49\pi^2)I_{th}$, and otherwise to zero. The corresponding bit-plane outputs are shown in (a'), (b'), and (c') of Fig. 7 with digital outputs of (1,1,1), (1,1,0), (1,0,1), (1,0,0), (0,1,1), (0,1,0), (0,0,1), and (0,0,0) in an orderly manner.

C. Pseudo-color:

From research results in optometry, it has been concluded that the human visual system can discriminate simultaneously only 15 to 20 gray levels from a complex black and white image. However, if the same image is presented in full color, the visually distinguishable levels can be increased enormously, up to hundreds or even thousands of different levels. Because of this increased resolution, techniques have been developed to encode color on black and white images such as radiographic, radioisotope scanning, and electron microscopic images. This encoding enhances the possibility of recognition or detection of the details of the images. The mapping of the black and white intensities into the three primary colors, i.e., blue, green, and red, is called pseudocolor encoding. This technique can definitely be used to enhance the acoustical holographic images.

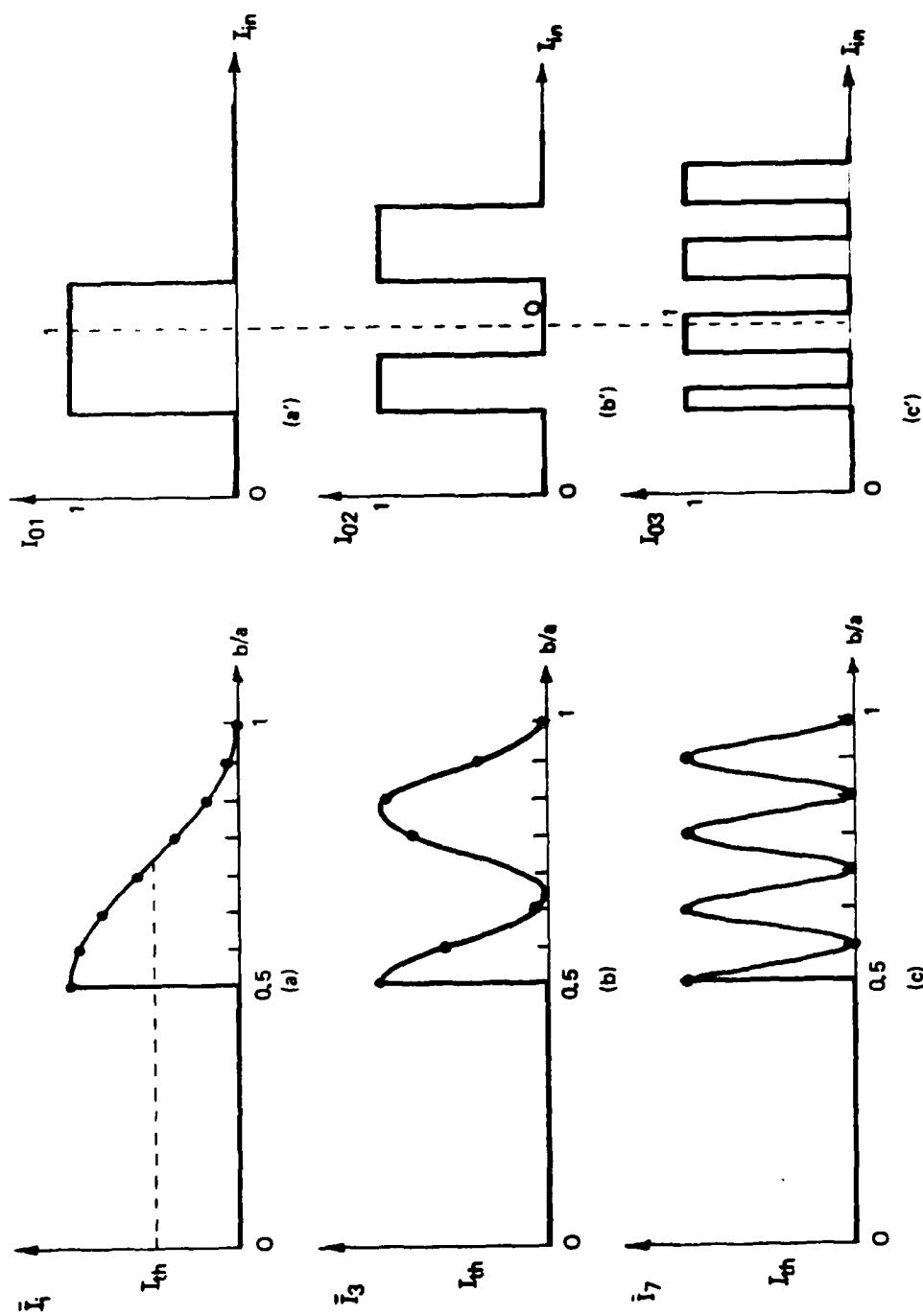


Figure 15. Illustration of how three-bit outputs, I_{01} , I_{03} , and I_{07} , are generated by a single contact screen photograph with eight different bar widths. These widths are $b/a = 0.5 + n/14$ for $n = 0, 1, 2, 3, 4, 5, 6$, and 7 . I_{th} is the detection threshold.

The basic principle of the new pseudo-color encoding process is selective mixing of the colored outputs of the high diffraction orders of a contact screen photograph or transparency in a coherent optical system. The contact-screen photograph is placed also in the object plane of a coherent optical system which has three colinear laser beams, each associated with a primary color. The pseudo-coloring of the picture can be achieved simply by selective mixing the high diffraction order outputs generated by each laser. White light source with color filters can also be used.

It is readily shown that the Fourier plane intensities for unit intensity input incident on the contact screen photograph may be expressed in a more detailed form by

$$\begin{aligned} I_n &= \left(\frac{b}{\lambda f}\right)^2 \sin^2 \left(\frac{n\pi b}{a}\right) \\ &= \frac{1}{\lambda^2 f^2} \frac{a^2}{n^2 \pi^2} \sin^2 n\pi b \end{aligned} \quad (34)$$

where λ is the wavelength of the laser, f is the focal length of the imaging lens, and n denotes a nonzero positive integer representing the order of diffraction.

In the coherent optical system, lasers of the three primary colors, blue (B), green (G), and red (R), are used, with their wavelengths respectively denoted by λ_B , λ_G , and λ_R , and collimated beam intensities expressed by I_B , I_G , and I_R . For each color, any desired diffraction order may be selected, and the three resulting color images can be recorded on a color film, or displayed simultaneously on a screen or by means of a color television monitor. If ℓ , m , and n denote the selected diffraction orders, the total intensity at a particular location of the output image, corresponding to the region where periodic opaque bars of width $(a-b)$ are found in the half-tone photograph, may be given by

$$\begin{aligned} I_t &= \frac{I_B a^2}{\lambda_B^2 f^2} \frac{1}{\ell^2 \pi^2} \sin^2 \frac{\ell \pi b}{a} + \frac{I_G a^2}{\lambda_G^2 f^2} \frac{1}{m^2 \pi^2} \sin^2 \frac{m \pi b}{a} \\ &+ \frac{I_R a^2}{\lambda_R^2 f^2} \frac{1}{n^2 \pi^2} \sin^2 \frac{n \pi b}{a} \\ &= \{I_{B\ell}\} + \{I_{Gm}\} + \{I_{Rn}\} \end{aligned} \quad (35)$$

where

$$I_{B\ell} \equiv \frac{I_B}{\lambda_B^2 f^2} \frac{a^2}{\ell^2 \pi^2} \sin^2 \frac{\ell \pi b}{a} \quad (36)$$

$$I_{Gm} \equiv \frac{I_G}{\lambda_G^2 f^2} \frac{a^2}{m^2 \pi^2} \sin^2 \frac{m \pi b}{a} \quad (37)$$

$$\text{and} \quad I_{Rn} \equiv \frac{I_R}{\lambda_R^2 f^2} \frac{a^2}{n^2 \pi^2} \sin^2 \frac{n \pi b}{a} \quad (38)$$

To illustrate the meanings of Eqs. (36)-(38) graphically, the functions $I_{B\ell}$, I_{Gm} , and I_{Rn} are plotted with respect to b/a ($0 \leq b/a \leq 1$) in Fig. 16 for $\ell = 1$, $m = 2$, $n = 4$, and pre-chosen values of I_B , I_G , and I_R . A particular value of $b/a = 0.4$ and its corresponding output intensities are marked as an example to show that the intensities of the three primary colors can be determined from these curves for a given region of the original picture. The net color, as a result of the mixture of these primaries, can be determined from a CIE chromaticity diagram. Naturally, the mixing of the three primaries does not have to be limited to the one-color-one-order assignment as given in Eq. (35). Any number of diffraction orders may be assigned to any color and different laser intensities may also be easily controlled by an attenuator. These features show that the new pseudo-color encoder has considerable flexibility.

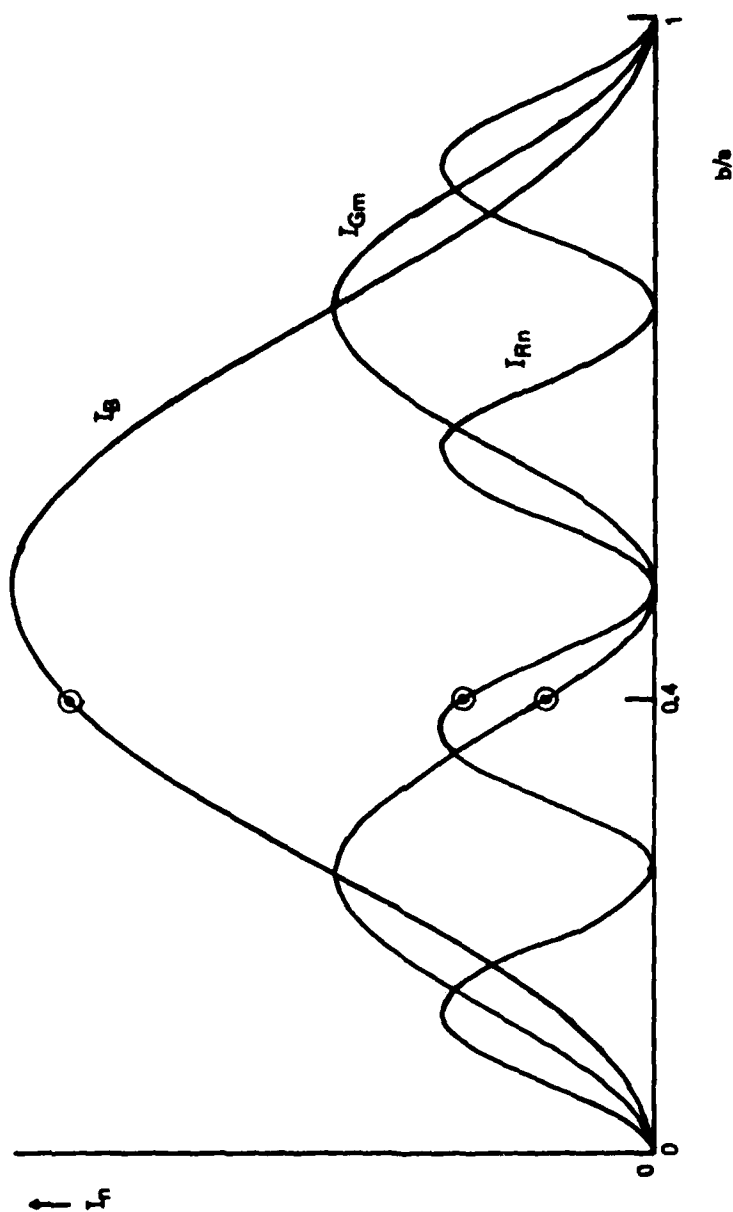


Figure 16. Intensity outputs I_B , I_{Gm} , and I_{Rn} versus b/a for $l = 1$, $m = 2$, and $n = 4$.

IV. Conclusion

A new acoustic wave memory device, its operating principle, and experimental results have been presented. The novelty of the device includes:

- (A) The AWMD can make real-time in situ recording, retention, and display of acoustic waves, the interference of the same, and acoustic holograms.
- (B) In the recording phase, heating of the thermoplastic material or any other material that can be softened by heat, first begins from the top layer of the material coinciding with the location where the recording of the acoustic information takes place. As a consequence, a relatively thick layer of thermoplastic material can be applied if necessary.
- (C) A variety of thermoplastic materials with different softening temperatures can be used in the device.
- (D) A variety of heating mechanisms can be used for the heating and softening of the recording material. For example, in addition to the electric resistive heating method described in Section II, a collimated beam of a heat lamp or an infrared laser can be applied to the top surface of the recording layer.
- (E) The size and shape of the AWMD can be tailored to fit into a variety of acoustic wave imaging systems.
- (F) The plexiglas support can be replaced by any other sturdy support that is transparent to acoustic waves of selected frequencies applied in a system.
- (G) If the electric heating is replaced by collimated radiation heating, any optically transparent top cover can be used to replace the electric resistive material coated quartz or heat resistant glass.
- (H) The top cover can protect the thermoplastic from getting contaminated by dust or other liquid (such as water) particles, and also keep the thermoplastic warm since the cover serves as a thermal insulator.

In addition, when the AWMD is modified by placing an ultrasonic diffraction grating immediately underneath the bottom of the device, the reference beam can be omitted and the test object can be placed directly under the device. This will increase the useful aperture of detection and the flexibility of the detection geometry.

Experimental results have shown the capability of these devices in achieving their desired objectives although more work will be needed for a refined device to satisfying realistic testing requirement.

For the enhancement of the acoustical holographic images, a few new coherent optical image processing techniques based on new contact screens have been presented. These techniques include equidensitometry, A-D conversion and pseudo-color. Not presented and still need-to-be studied is the technique of logarithmic filtering which can remove the multiplicative noise in the image from the signal and thus greatly enhance the signal-to-noise ratio and the resolution of the images. The main advantage of optical over the existing digital technique is processing speed. Therefore, real-time optical spatial filtering techniques should be studied for the improvement of the acoustical images.

In addition, future work in getting the quantitative data on the diffraction efficiency, resolution, recording time, memory time, recording temperature, erasing temperature, recording sensitivity, substrate thickness, and recording medium thickness should be investigated before the device can be well-designed. Thermal sensitive materials such as Criscool used in the experiment reported should also be explored for the device and ultrasonic grating structures should be studied as well.

Once the device is made practical, it has great potential in HNDT for military, industrial, and medical applications.

References

1. Young, J. D. and Wolfe, J. L., "A New Recording Technique for Acoustic Holography," *Applied Physics Letters*, Volume 11 (1967), p. 294.
2. Liu, H. K., "A Thermoplastic Device for Real-Time IN-SITU Recording of Acoustic Holograms," Technical Report RI-80-4, U.S. Army Missile Command, Redstone Arsenal, AL 35809 (October, 1979).
3. Liu, H. K., "Acoustic Holographic Image Storage and Its Coherent Optical Reconstruction," *Proceedings of the Optics in Four Dimensions International Meeting (CICESE)*, Ensenada, Baja California, Mexico, (August, 1980).
4. Liu, H. K. and Schaeffel, J. A., "Real-time Recording, Display and Retention of In-line Acoustic Holograms," *SPH-8 Huntsville Electro-Optical Technical Symposium*, Vol. 255 (1980).
5. Green, P. S., "A New Liquid-Surface-Relief Method of Acoustic Image Conversion," *Acoustic Holography*, Plenum Press, Volume 4 (1972), 173.
6. Liu, H. K., "Halftone Screen with Cell Matrix," U.S. Patent No. 4188225, Feb. 12 (1980).
7. Liu, H. K., "Method of Producing Contour Mapped and Pseudo-Colored Versions of Black and White Photographs," U.S. Patent No. 4207370, June 10 (1980).

DISTRIBUTION

	<u>No. of Copies</u>
Defense Technical Information Center Cameron Station Alexandria, VA 22314	12
IIT Research Institute ATTN: GACIAC 10 West 35th Street Chicago, IL 60616	1
US Army Materiel Systems Analysis Activity ATTN: DRXSY-MP Aberdeen Proving Ground, MD 21005	1
DRSMI-LP, Mr. Voigt	1
-EX, Mr. Owen	1
-R	1
-RPR	3
-RPT (Record Copy)	1
(Reference Copy)	1
-RL	10

DATE
ILMED
-8